

Article

Product design driven by biosensors: Improving interactivity and user experience

Jianhai Shi^{1,2,*}, Irwan Syah Md Yusoff³, Mohd Faiz Bin Yahaya⁴¹ Jinan Engineering Polytechnic, Jinan 250200, China² Faculty of Design and Architecture, University Putra Malaysia, Serdang 43400, Malaysia³ Faculty of Human Ecology, University Putra Malaysia, Serdang 43400, Malaysia⁴ Faculty of Design and Architecture, University Putra Malaysia, Serdang 43400, Malaysia* **Corresponding author:** Jianhai Shi, jianhai8336@163.com

CITATION

Shi J, Yousoff ISM, Yahaya MFB.
Product design driven by biosensors:
Improving interactivity and user
experience. *Molecular & Cellular
Biomechanics*. 2025; 22(4): 1028.
<https://doi.org/10.62617/mcb1028>

ARTICLE INFO

Received: 6 December 2024

Accepted: 3 January 2025

Available online: 4 March 2025

COPYRIGHT



Copyright © 2025 by author(s).

Molecular & Cellular Biomechanics
is published by Sin-Chn Scientific
Press Pte. Ltd. This work is licensed
under the Creative Commons

Attribution (CC BY) license.

<https://creativecommons.org/licenses/by/4.0/>

Abstract: Product design has increasingly become the process of creating stronger relationships between people and products while improving utility and emotional involvement in today's fast-paced technological environment. Biosensors that measure physiological and neurological responses have been revolutionary tools in this field. To establish the biosensor-driven design methodology to enhance interactivity and user experience in cultural and creative product design. The device employs electroencephalography (EEG), a sophisticated biosensor, to capture users' emotional states and preferences as they interact with various cultural elements. The pleasure-arousal-dominance (PAD) model is used to evaluate EEG data. To extract consumers' perceptual image semantics for product design, factor analysis is used concurrently. An Intelligent Sea Lion Optimization (ISLO), combined with a Resilient Long Short-Term Memory (RLSTM), evaluates user interaction, reducing fatigue from repeated interactions. Designers employ cultural factors to inform the first product prototypes, and the system iteratively refines ideas by matching them to the emotional demands of users. The results indicate the effectiveness of integrating user feedback into interactive design processes. As a result, the ISLO-RLSTM method performed better in RMSE at 1.58, MAE at 1.22, and MSE at 2.17. This approach demonstrates the way biosensors can revolutionize product creation and improve user experiences by bridging the gap between functional design and emotional engagement.

Keywords: product design; biosensors; interactivity; user experience; intelligent sea lion optimized resilient long short-term memory (ISLO-RLSTM)

1. Introduction

Sensors are excellent information-gathering devices for the deployment of smart towns because of their unique position at the interface between the analog world humans live in and basic communication organizations. Depending on the application context, sensors are characterized as physical or virtual. Biosensors play a significant role in product design, having progressed from traditional electrochemical biosensors to wearable and implantable biosensors [1]. Biosensors are a popular topic in today's scientific community. With advancements in science and technology, biosensors have become more sensitive and capable of detecting biomolecules in various fields, including medical, environmental, and military [2].

A biosensor is a device able to convert chemical data derived from biomolecule concentrations into usable analytical signals. It essentially constitutes four constructions consisting of elements of the sensing bind, which exactly binds with

the analyte being tested, an interface offering a working location for the elements of a biosensor, converting chemical or physical data, resulting from the collaboration between the elements of sensing with the analyte in the electrical signals, and amplification and processing of these signals together with an interface circuit designed for data processing and analysis. The biosensor's structure is represented in **Figure 1** [3].

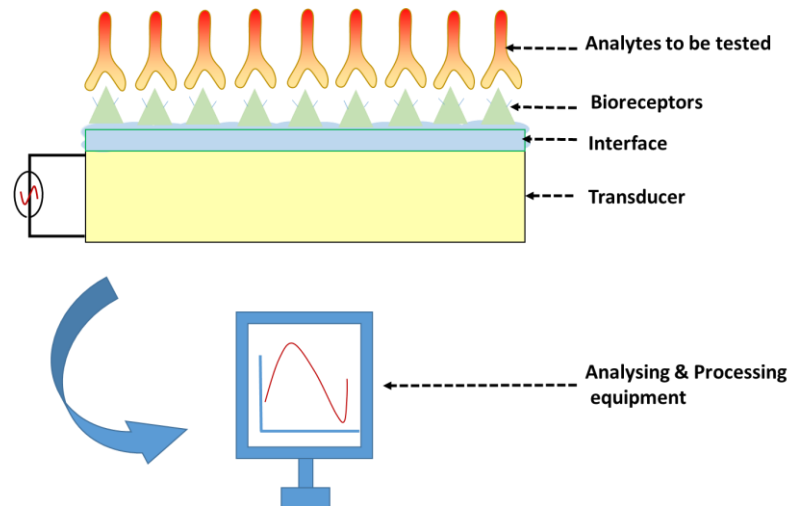


Figure 1. Biosensor's structure.

The term “biosensor” is derived from two words: “bio”, an abbreviation for biology or life, and sensor, indicating a device or system that measures and responds to stimulant. A biosensor is a highly advanced analytical instrument that has been precisely designed to detect subtle changes occurring within complex biological processes, an essential feature in product design. It converts these small fluctuations into recognizable electrical signals. At the core, this biosensor utilizes the synergistic interaction of this biological sensing element with a transducer, itself an integral part of the conversion of biological information into measurable electrical signals [4]. Biosensors are low-cost and portable devices that can detect pathogens, proteins, and other analytes in a matter of instant time; establishing new possibilities for innovation in product design. They intend to eliminate the time and high cost of expertise involved in testing processes that, in certain industries, cost more to acquire. Biosensors form a rapidly developing multidisciplinary field, potentially transforming consumer, health care, and industrial testing [5].

These devices have provided solutions to a variety of applications, including food safety and processing, drug growth, disease detection, defense, biomedicine, environmental monitoring, and security [6]. Biosensors are designed based on the target analyte and transduction process, the characterized as labeled or label-free based on their label use. Labeled biosensors utilize a reporter for identifying analytes such as enzymes, electroactive chemicals, or fluorescent molecules. Labels improve signal amplification and selectivity for sensing but occur at a higher cost and longer sensing time. Label-free approaches rely on bio recognition elements (BRE) to recognize targets, and their basic design makes them ideal for portable devices and adaptable in product design [7].

According to the traditional definition, biosensors are sensors that make use of a bio receptor, such as nucleic acid, peptide, enzyme, antibody, etc. Biosensors have developed into many different kinds of transducers, such as spectroscopic, optical, and electrochemical biosensors [8]. In today's rapidly developing technology environment, product design prioritizes strengthening links between people and things to improve usefulness and emotional involvement. Biosensors can measure physiological and neurological responses, making them a game changer. This research aims to develop a biosensor-driven design approach to improve interaction and user experience in creative and cultural product design.

Contribution of the research

- The use of EEG biosensors to record emotional reactions gives designers of customized products access to real-time data. Users are more emotionally invested in items as a result of this integration.
- Using EEG data and the PAD model, a novel strategy was presented for enhancing user involvement and emotional engagement in cultural and creative products. Product experiences become more meaningful as a result.
- To improve the entire design process by reducing interaction fatigue and enhancing design prototypes, factor analysis, Intelligent Sea Lion Optimization (ISLO), and Resilient Long Short-Term Memory (RLSTM) are used.
- To ensure that product prototypes reflect the feelings and preferences of users, the technique incorporates cultural components into the design process. This encourages more enticing and pertinent cultural product designs.

The organization of the research involves the following structures: Section 2 provides the related works and the methodology is explained in section 3. The result of the research was evaluated in Section 4 and discussed briefly in section 5. Section 6 covers the conclusion.

2. Related works

The state of the art for several smartphone-based biosensor types was provided, considering their stages of development in Madrid et al. [9]. A comprehensive examination of the potential causes of the failure of several innovations to make it to market was provided in the second section. The result highlighted the necessity of bolstering the phases of technology transfer, application, and end-user acceptance. By considered nanophotonic' potential in biosensing, compiled current developments in the creation of optical and nanophotonic biosensors, emphasizing their sensing capabilities [10]. They usually divide these kinds of biosensors into five groups: surface-enhanced spectroscopies, phase-driven, resonant dielectric nanostructures, plasmonic, and evanescent-field. Evaluated the significance of improving the performance and effectiveness of the sensor by tackling some of the main issues in nanophotonic biosensing, like resolving the problems of managing biological specimens and reducing their costs for accessibility.

An rise in emotional and physical self-awareness was brought about by the upgrading of affective technologies [11]. It described the bio signals used in inexpensive physiological monitoring and how they might be integrated with the

techniques of interface designers to create aesthetically pleasing and physiologically engaging experiences. The term orchestration was presented, which refers to the process of creating the entire interaction, including the coupling of sensors, starting and stopping the interaction, habituating, and modifying the relaxing, soothing, or stimulating impacts of the interaction. A comprehensive overview of the various machine learning (ML) techniques used in food safety biosensors was provided by Zhou et al. [12]. The main ML techniques were first described, and then a detailed investigation of the combined use of biosensors and ML in food safety was conducted. The results showed that ML-based algorithms could help to identify food safety problems quickly. To evaluate food quality, Zhu [13] showed how to integrate biosensors with deep learning (DL). They initially concentrate on the datasets required to train the models and the procedure by which deep neural networks (DNN) produce prediction models. Second, they highlight research on biosensors for food nutritional content measurement and how convolutional neural networks can be used to extract exterior aspects of food products.

The applications of surface enhanced raman spectroscopy (SERS) and ML in the last years included the identification of biological molecules, rapid detection of diseases, development of new methods for immunoassay, and improvement of the performance of SERS in semi-quantitative measurements [14]. At the end, the possible benefits and challenges of integration between SERS and ML were addressed. Anapanani [15] evaluated the use of ML in biosensors, which pointed out potential benefits of this technology, including increased sensitivity, selectivity, and accuracy. It covered various ML methods applied in biosensors, including feature extraction, data preparation, and classification models. Challenges of integrated ML with biosensors, including issues related to data accessibility, functionality of sensors, and processing demands. The use of ML in improving the performance of these bioreceptor-free biosensors Schackart et al. [16] discussed the ML has been applied to imaging, Etongue and Enose, as well as SERS-based biosensors.

Significantly, principal component analysis (PCA) combined with support vector machine (SVM) and various artificial neural network (ANN) algorithms performed well in a range of tasks. DL neural network (DLNN) was developed to classify gait and assess the joint angle, based on sEMG signals as well as filtered and denoised signals from sEMG and plantar pressure measurements acquired during human walking [17]. The findings show high precision for joint-angle computation and distinguishing human gait with the best accuracy as 95.42%, the lowest of 90.11%, and an average error of 3.19 for joint angle estimate. The multifaceted uses of ML models, such as regression and classification, and how they raise the potential of biosensors were examined [18]. To examined at great length the functions of wearable sensors, colorimetric sensors, electrochemiluminescence/chemiluminescence sensors, lab-on-a-chip sensors, and ML-assisted electrochemical sensors in analysis. A plan to ascertain and predict the sample rate of active biosensors in wireless body area networks (WBANs) was presented [19]. Three primary factors were used in the scheme: patient activity, risk, and pivot biosensor value. Additionally, the Spline interpolation method and a modified Fisher test were employed. After every cycle, the sampling rate was calculated using mathematical and statistical techniques. Two ML methods, adaptive

neuro fuzzy inference system (ANFIS) and long short-term memory (LSTM), were used to forecast the sample rate after a certain round has been reached. The suggested methods cut network energy use by 73% and data traffic by 81%.

Hemdan et al. [20] looked at a variety of biosensor technologies, including enzymatic, immunological, and deoxyribonucleic acid (DNA) sensors, as well as how they are used in disease biomarker detection and drug monitoring. Recent advancements like wearable technology and the incorporation of nanotechnology were emphasized, and issues like data confidentiality, repeatability, sensitivity, and specificity were discussed. It improved global healthcare results, stimulated technology innovation, and guided strategic decision-making. The relevant research progress of nanozyme-based biosensors for organ phosphorus pesticides (OP) detection was compiled in Zhao et [21]. It includes a discussion of the biosensing approach, catalytic activity, and structural categorization. The research presents the practical uses of nanozyme-enabled biosensors, such as optical and electrochemical biosensors, with a focus on on-site detection, low cost, and ease of use. Lastly, the primary issues and potential developments are discussed, which can offer theoretical support for the use of nanozyme-based biosensors in organophosphorus pesticides (OP) detection. Inshyna et al. [22] examined the composition, classification, and applications of modern biosensors in a number of fields, with a focus on design advancements and bioreceptor immobilization methods. It compares immobilization techniques, examined the use of metal nanoparticles and carbon nanomaterial's to improve electrochemical characteristics, and evaluates optical, acoustic, calorimetric, piezoelectric, and electrochemical sensors. The usefulness of immobilization techniques and their uses in environmental monitoring, human health diagnostics, and the evaluation of food and water quality are also covered.

3. Methodology

The section consists of some of the following procedures. The chair and teapot data were gathered and then the PAD model was used to evaluate EEG data. Next, factor analysis is used concurrently to extract the semantics of the perceptual image of consumers for product design. Finally, an ISLO was combined with an RLSTM to evaluate user interaction, reducing fatigue from repeated interactions. **Figure 2** depicts the architecture of the methodology.

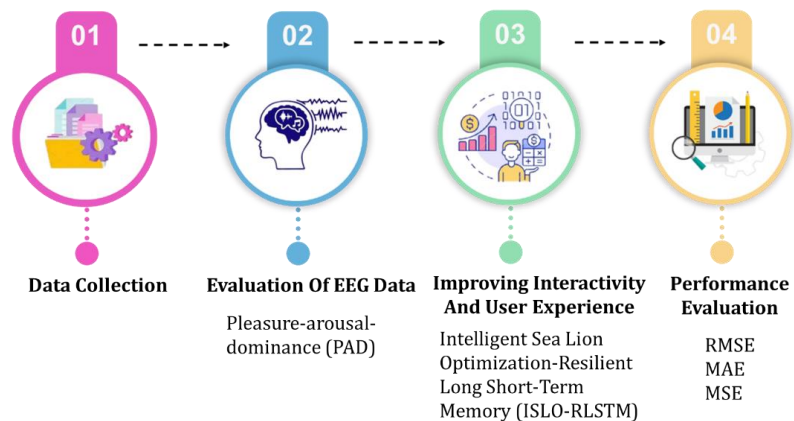


Figure 2. Architecture of the methodology.

3.1. Data collection

The data was gathered from the open source Kaggle website: <https://www.kaggle.com/datasets/ziya07/biosensor-driven-product-design/> data. This dataset is a user interaction data with cultural and creative products, like chairs, tea cups, etc. The dataset is merged together EEG signals with user feedback measurements of user satisfaction and emotional engagement during product interaction. The dataset contains EEG signal data of different brain wave frequencies, such as beta, theta, delta, alpha, and gamma, which have been captured during user interaction with a product. As the goal variable, the satisfaction ratings are utilized to group users into three satisfaction levels: high, medium, and low.

3.2. PAD model

The model pleasure-arousal-dominance (PAD) is widely applied to product design to evaluate the emotional response and enhance the user experience by measuring levels of pleasure, arousal, and dominance during contact. Biosensors are integrated with this model to provide immediate feedback on consumers' states of mind, allowing designers to develop more engaging and tailored products. This approach enhances interaction because it matches the properties of the product with consumer emotional responses, thereby creating higher pleasure and usefulness.

3.2.1. Emotional scale of PAD model

The PAD emotion scale has strong structural validity and can reliably assess emotional state based on three dimensions: dominance, arousal, and pleasure. Therefore, the PAD emotion scale was utilized to gauge users' feelings regarding various cultural components. Eight categories can be determined by the three dimensions mentioned above, such as $+P - A - D$ (gentle), $-P - A - D$ (boring), $+P + A + D$ (happy), $+P + A - D$ (dependent), $+P - A + D$ (relaxed), $-P - A + D$ (disdainful), $-P + A - D$ (anxious), and $-P + A + D$ (hostile). The six pairs of adjectives that make up the PAD emotion scale each indicate a various emotional state, with each pair of adjectives representing a dimension as depicted in **Figure 3**.

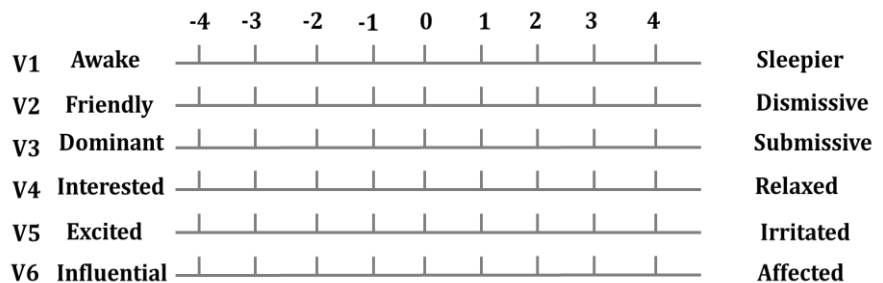


Figure 3. PAD model's emotional scale.

Every pair of adjectives indicates the opposite emotions on the dimension to which they are connected, even if the emotional values on the remaining two dimensions are nearly identical. The semantic distinction scale with a score of nine is used to assess these feelings. For instance, V1: awake-sleepier has a score in the

range of -4 to 4 . The subjects' emotional intensity determines their score. The "awake" score increases as it moves from left to right. The more precise the score, the "sleepier" the condition it depicts. The correlation between the scores of the aforementioned six pairs of adjectives, pleasure (P), arousal (A), and dominance (D) is demonstrated by Equations (1) to (3). Each dimension's score is calculated as the average of the four adjective groups.

$$P = \frac{(V1 - V2 + V4 - V5)}{4} \quad (1)$$

$$A = \frac{(-V2 + V3 - V4 + V6)}{4} \quad (2)$$

$$D = \frac{(V1 - V3 + V5 - V6)}{4} \quad (3)$$

3.2.2. PAD model's emotion test

Subjects rated the six objects in **Figure 3** on a scale from -4 to 4 for each of the two images. The two categories into which the two image samples were split: like and dislike. To generate distinct emotional experiences from the patients, three sets of image samples representing various emotional states were used as the visual inducement materials for the next EEG tests. The PAD model enabled exact classification of the emotional state as it measured pleasure, arousal, and dominance, which were required to be measured for biosensor-based analysis. EEG data collected from this test was further analyzed using ISLO-RLSTM to determine the user interaction that ensures an emotional fit with product design. Factor analysis reduced perceptual image dimensions, streamlining cultural elements for higher design accuracy. This method fills the gap between users' emotional needs and functional product design, enhancing interactivity and user experience.

3.3. Experimental data analysis

The gathered information was examined using the Bio semi Active Two, which is an EEG system that was employed for the acquisition of high-quality data of neurophysiological. Signals that were elicited by image presentation were obtained at 5000 ms. The EEG data obtained were processed digitally, then segmented and operated. For quantitative analysis, the average power of α wave was measured at electrodes F_{P1} , F_{P2} , F_3 , F_4 , F_Z , C_Z , and P_Z in the frequency range 8~13 Hz. No significant difference in the average power of α waves at F_{P1} (left frontal pole), F_3 (left frontal), and F_{P2} (right frontal pole), F_4 (right frontal) under general stimulation. The preferred images reduced the mean power of the α waves in the F_3 and F_{P1} , meaning that these images evoked positive emotions among the users.

When respondents were exposed to disliked images, the average strength of the wave in the right frontal pole decreased, indicating that these images triggered negative feelings. **Table 1** examines the strength of α waves in the F_{P1} and F_{P2} following stimulation with various image samples. The difference in the strength of the α wave in the F_{P1} and F_{P2} helps to measure a subject's emotional state, offering designers with user preferences through emotion.

Table 1. Power of α waves in F_{P1} and F_{P2} analyzes.

Number of the Image	F_{P1}	F_{P2}	F_{P1}/F_{P2}	Features
1	3.562	4.245	0.84	Like
2	4.158	3.465	1.20	Dislike

3.4. Perceptual image semantics' factor analysis

The factor analysis was applied to reduce a few complete image vocabularies from the perceptive component. Exploratory factor analysis (EFA) was applied to the relationship between variables. The EFA value was close to one, and the correlation between the variables was higher. If the EFA measure is greater than 0.7, then this analytic approach can be used. This method reduces the dimensionality while retaining essential perceptual attributes. Moreover, EFA also helps in uncovering the latent patterns within the data, thereby enhancing the interpretability of the perceptual image semantics. This approach refines the relationship between the user emotions and the product design to deliver more focused and impactful results.

3.5. Improving interactivity and user experience using an intelligent sea lion optimization -resilient long short-term memory (ISLO-RLSTM)

The proposed ISLO-RLSTM model to optimize and improve biosensor-driven systems. ISLO boosts resilience by determining ideal settings for consistent performance in a variety of situations, while RLSTM efficiently analyzes time-series biosensor data and models user interactions in real time. ISLO-RLSTM improves product flexibility via sensor feedback, resulting in more customized and responsive experiences. ISLO-RLSTM forecasts trends and dynamically adjusts product behavior, enhancing engagement and user experience.

3.5.1. RLSTM

To create an RLSTM model that makes predictions about a user's emotional and physical states in real time based on biosensor data. As shown in **Figure 4**, $E = \{y^{(0)}, y^{(1)}, \dots, y^{(m)}\} (y^{(j)} \in R, j \in [0, m])$ represents the sensor data generated by the biosensors, which track a user's emotional states over time, such as pleasure and arousal. A n -dimensional vector of physiological measures from m sensing channels, including EEG signals, is represented by each data sample $y^{(j)}$. Let l_y and l_z represent the input and predicted sequence lengths, respectively, for the RLSTM model. The prediction issue is formulated as follows: The model generates $Z = \hat{z}^{(t)}$, which is the expected emotional state or interaction outcome at time t , given the input $Y = y^{(t-l_y)}, y^{(t-l_y+1)}, \dots, y^{(t-1)}$. To simplify the model and focus on precise, real-time predictions, employ $l_y = 1$.

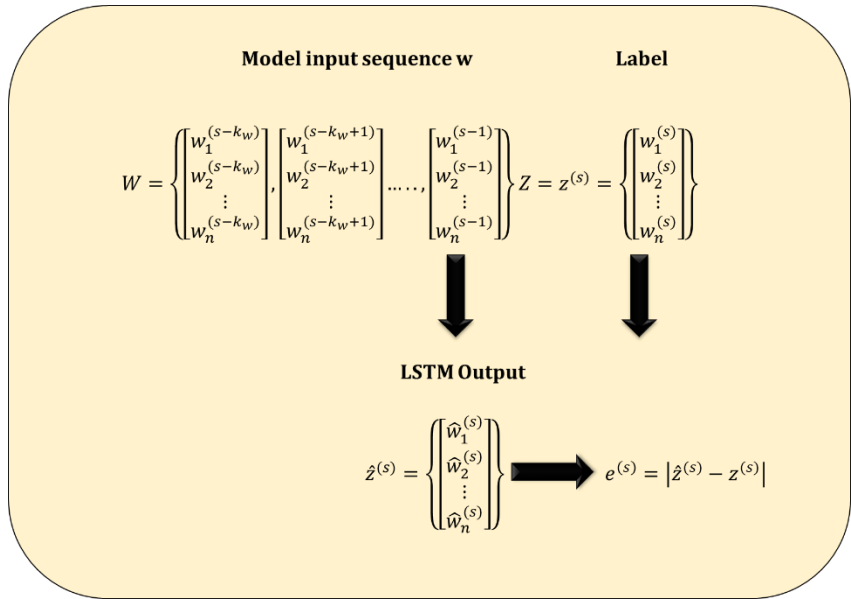


Figure 4. Prediction of user interaction in biosensor.

The fundamental challenge in the creation of an RLSTM model in user interaction prediction of product design driven by biosensor data is the variability in physiological data from different users and interactions. Physiological signals may vary widely depending on the user’s preference, the situation, or the way they interact with the product. Other signals, for example, pulse rate, are likely to be steadier in pattern, while a user’s emotional response to the qualities of a product, say visual attractiveness or haptic feedback, is likely to vary hugely depending on their mood. The primary objective of an augmented RLSTM model is to predict user engagement and emotional reactions accurately, while accounting for the wide variation in physiological signals between different users and situations. This makes the model better suited for application to a range of product designs and usage conditions. **Figure 5** illustrates the structure of the RLSTM model.

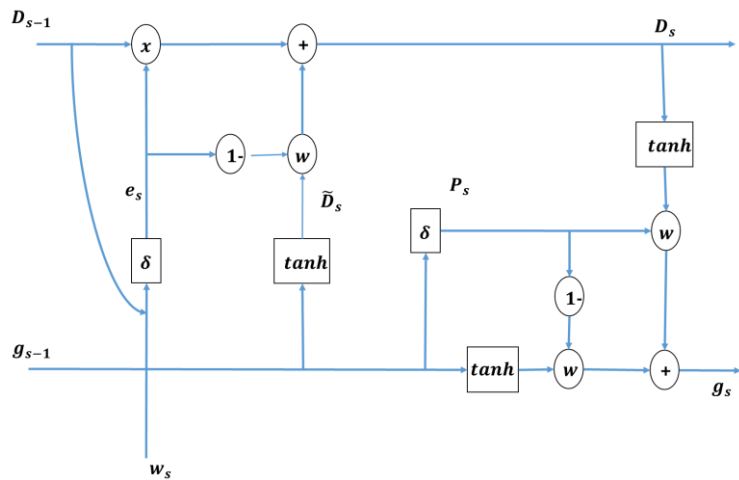


Figure 5. Structure of RLSTM.

Unlike traditional LSTM models, the RLSTM model’s input gate incorporates both the input and forget gates. When users’ emotional states or interactions are

influenced by prior experiences or context, this design enables the model to update the cell state based on new inputs while retaining critical historical data. The updated model can be characterized using the following Equations (4) to (6).

$$e_s = \delta(W_e \times [y_s, g_{s-1}, D_{s-1}] + c_e) \quad (4)$$

$$\widehat{D}_s = \tanh(W_d \times [y_s, g_{s-1}] + c_d) \quad (5)$$

$$s = D_{s-1} \times e_s + \widehat{D}_s \times (1 - e_s) \quad (6)$$

where y_s is the current input (e.g., physiological measurements), g_{s-1} is the previous hidden state, and D_s is the updated cell state. The present input y_s has a greater effect on capturing real-time changes in the user's emotional and physiological state. The expected emotional or interaction state of the user is calculated as following Equations (7) to (9).

$$P_s = \delta(W_o \times [y_s, g_{s-1}] + c_o) \quad (7)$$

$$Q_s = \tanh(W_q \times [y_s, g_{s-1}] + c_q) \quad (8)$$

$$g_s = P_s \times \tanh(D_s) + (1 - P_s) \times Q_s \quad (9)$$

After training the RLSTM model with biosensor data from user interactions, it is used to anticipate user reactions in real time while using the device. The model predicts the value $\hat{z}^{(t)}$ for each time instant s using the input sequence $Y = y^{(t-l_y)}, y^{(t-l_y+1)}, \dots, y^{(t-1)}$. The anticipated emotional or physiological state $\hat{z}^{(t)}$ is then compared against the actual observed values to compute an error $e(t) = |\hat{z}^{(t)} - y(t)|$. RLSTM detects a substantial change in user interaction or emotional reaction, suggesting a possible problem with the product design or user experience, if the error is beyond a predefined threshold T_e , i.e., $e(t) > T_e$. A crucial factor in guaranteeing the model's sensitivity to variations in user involvement is the error threshold T_e , which affects how well real-time feedback works for interactive product design.

3.5.2. ISLO

The ISLO was used, which can improve product design by optimizing biosensor integration, increasing user interface engagement, and fine-tuning the user experience using adaptive algorithms. It can effectively pick the best sensor setups, resulting in more responsive and tailored goods. ISLO's optimization approach speeds the iterative design process, allowing for real-time revisions depending on user feedback. This results in novel designs that are more intuitive and user-centered, which improves the whole product experience.

1) Improvement of the Exploration phase

Due to the inheriting characteristics of current solutions, newborn agents result in poor exploration search capacity throughout the ISLO exploration phase. To address this issue, a newly developed solution should satisfy two criteria:

- Carrying random features to guarantee a robust exploration phase capability.

- Landing in a sufficiently respectable position. To increase the performance, a new, enhanced operation is implemented that takes advantage of both the individual's history and the best global answer.

The idea of a person's past data comes from particle swarm optimization (PSO), including the bird swarm algorithm and the gaining-sharing knowledge algorithm. The second criterion is guaranteed by a piece of information from the world's finest information, whereas the first requirement for the recently updated answer is guaranteed by knowledge about a person's past with a random coefficient. Combining three vectors allows new ways to the global best solution (GBS), the best distinct tests, and the search space. In keeping with that idea, Equations (10) to (12) suggest the following new update method in ISLO to enhance exploitation possibilities.

$$dif_1 = (2r_1 Y_{best}^h - Y^h) \quad (10)$$

$$dif_1 = (2r_2 Y_{best}^h - Y^h) \quad (11)$$

$$Y^{h+1} = Y^h + D \times dif_1 + D \times dif_2 \quad (12)$$

where Y^h local represents the individual's best position up to iteration h , r_1 and r_2 are random numbers in the interval $[0, 1]$, dif_1 is the difference between the current position and the best solution discovered thus far, and dif_2 is the difference between the current position and the best solution discovered throughout the current individual's history. In a few iterations, especially with the value D , Equation (12) focused on the search procedure with more data from both vectors, which will help the algorithm to know the most probable location in a larger jump. The effects of both factors are defined by two random numbers, r_1 and r_2 . Additionally, they are essential to the updating process since they produce random characteristics for the operation, which enables ISLO to utilize both considerations and avoid the local minimum. When r_1 and r_2 are absent, the reorganized location is continuously impacted by the similar proportion of the best representative and its experience throughout generations, which reduces population diversity.

2) Improvement of the Exploitation phase

According to the observations, ISLO takes benefits of the GBS while roaming about to produce fresh, untapped options. As a result, the algorithm's exploitation potential in multidimensional space is limited, as the genuine GBS can exist in the opposite direction of the present GBS. The RLSTM method enables ISLO to conduct faster searches during exploitation. RLSTM has been effectively applied to grasshopper optimization algorithms, grey wolf optimization, and other applications. First, Equation (13) improves exploitation. Because of the large value of D , the generated result jumps in a limited range around the Y_{best} solution, and the normal variable D guarantees that the newly produced result is broken in an arbitrary direction for every generation.

$$Y^{h+1} = Y_{best} + D N(0, 1)(2r_3 Y_{best} - Y^h) \quad (13)$$

Following that, RLSTM is used to generate the opposite solution (Equation 14) of the previously generated solution. As a result, ISLO searches for both the opposite

and present positions using the GBS at the same time, allowing ISLO to exploit more quickly and effectively.

$$Y_{oppo}^{h+1} = LB + UB - Y_{best} + r_3(Y_{best} - Y^{h+1}) \quad (14)$$

ISLO-RLSTM technique enhances product design through biosensors, bringing in interaction and satisfaction among customers. The improvement in parameters of RLSTM increases predictions about user preferences based on biosensor inputs accurately, and its adaptive learning enables strong robustness to fluctuations in inputs. This technique also lowers the processing cost as its parameter adjustment is optimized and provides real-time responses and smooth interaction with interactive systems. ISLO-RLSTM also enhances system stability, enabling the effective regulation of noise and uncertainty in sensor data. With its ability to be applied to various biosensor types, it thus expands its application in a wider range of product designs. More importantly, the method fosters innovation by accommodating more customized and adaptive experiences for users. Algorithm 1 illustrates the pseudocode for the proposed ISLO-RLSTM approach.

Algorithm 1 ISLO-RLSTM

```

1: Input Parameters:  $t_{max} = 1000, N = 50, D = 30, l_y = 1, T_e = 0.5$ 
2: Initialize agents and best solutions:  $Y_{best}, Y_h, g_{best}$  and  $g_h$ 
3: Initialize random numbers for exploration:  $r_1, r_2$  and  $r_3$ 
4: # RLSTM model initialization
5: for  $h$  in  $\text{range}(t_{max})$ :
6: # Exploration phase
7:   for  $i$  in  $\text{range}(N)$ :
8:     Update difference for exploration based on a GBS using Equation (10)
9:     Update difference for exploration based on historical best solution using Equation (11)
10:    Update the position of agents based on  $dif_1$  and  $dif_2$  using Equation (12)
11:    Update global best solution
12:     $Y_{best} = \text{np.min}(Y_h, \text{axis} = 0)$ 
13: # Exploitation phase
14: for  $h$  in  $\text{range}(t_{max})$ :
15:   for  $i$  in  $\text{range}(N)$ :
16:     Update solution in exploitation using a random walk around global best solution using Equation (13)
17:     Update solution based on the opposite direction of the global best solution using Equation (14)
18:     Update the GBS after the exploitation phase
19:      $Y_{best} = \text{np.min}(Y_h, \text{axis} = 0)$ 
20: # ISLO optimization of user interaction (input: physiological measures)
21: Calculate the error gate using Equation (4)
22: Calculate the candidate's memory using Equation (5)
23: Update the cell state using Equation (6)
24: Update the output gate using Equation (7)
25: Calculate the alternative candidate using Equation (8)
26: Update the final state using Equation (9)
27: #RLSTM for interaction errors
28:    $\text{error} = \text{np.abs}(g_s - \text{actual\_state})$ 
29:   if  $\text{error} > T_e$ :
30:     pass
31: Output Parameter: The best solution found after both the exploration and exploitation phases, represented by
32:  $Y_{best}$ 

```

4. Result

4.1. Experimental setup

To ensure effective processing of complicated data, the experimental setup uses Python 3.9 in the Anaconda environment on a high-performance workstation equipped with an NVIDIA GeForce RTX 3070 GPU, AMD Ryzen 9 5900X CPU, 32 GB RAM, and 1 TB SSD.

4.2. Analyzes of user perceptions images of cultural and creative products

A total of nine adjectives were gathered from various sources, including the internet and publications, to describe the image of cultural and creative items, as represented in **Table 2**. The flavoring chair and teapots were designed with distinct shapes and styles to broaden customers' awareness of chair and teapot shapes. Image vocabulary consists of responsiveness, user adaptability, real-time feedback, personalization, innovation, functionality, durability, cost-effectiveness, and simplicity.

Table 2. Image vocabulary.

Image vocabulary	
1	Responsiveness
2	User Adaptability
3	Real-time Feedback
4	Personalization
5	Innovation
6	Functionality
7	Durability
8	Cost-effectiveness
9	Simplicity

The observed value in Mauchly's test of sphericity could be interpreted as signifying a substantial difference between the unit matrix and the correlation coefficient matrix because the corresponding probability of the $P - value$ was near zero and below the significance level of α ($\alpha = 0.05$). The selection of words with high load factor values from each group was used to determine users' image desire for cultural and creative things. These language terms included exceptional texture, unique style, inventiveness and intrigue, practicality, and simplicity. The dimension of the nine variables was reduced to four factors in the way described above, which allowed for the reflection of most of the information from the original variables. 3 handle features of the teapot, 3 body features of the chair, and 6 decorative patterns were attained in **Table 3**. By randomly combining the system, six chromosomes were created. **Table 4** displays the initial population of flavoring chair and teapot shapes and matching codes that were produced at random.

Table 3. Characteristics of the flavoring chairs and teapots.

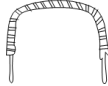
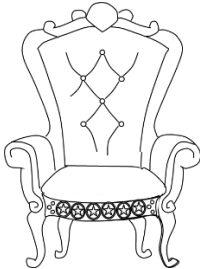
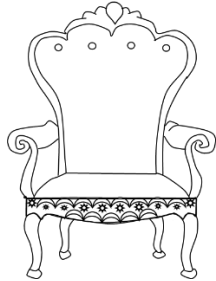
Characteristics	Shapes and Patterns		
Body Features of Chair			
Decorative Patterns of Chair			
Body Features of Teapot			
Decorative Handle Patterns of Teapot			

Table 4. Initial population of flavoring chairs and teapots.

Characteristics	Flavoring Chairs and Teapots		
Body Features of Chair			
Decorative Patterns of Chair			

Each column's bolded data in **Table 5** indicates a heavier stress on one of four elements, accordingly. For example, the first element can explain classical, fashionable, and five perceptual image vocabularies. Thus, the general style type of creative and cultural products is primarily explained by the first factor; users' demands for engaging and customized design are primarily reflected by the second factor; the high-quality design of the details of the product's cultural and creative is primarily explained by users' expectations in terms of the third factor; and users' consumption tendencies are primarily reflected by the fourth factor.

Table 5. Rotated component matrix.

Components	1	2	3	4
Responsiveness	0.845	-0.112	0.215	0.034
User Adaptability	0.812	0.021	0.123	-0.198
Real-time Feedback	0.745	0.105	-0.098	0.198
Personalization	0.153	0.872	-0.113	-0.089
Innovation	-0.011	0.854	0.192	-0.135
Functionality	-0.043	0.209	0.798	0.093
Durability	0.121	-0.134	-0.109	0.882
Cost-effectiveness	-0.015	-0.098	0.124	0.855
Simplicity	0.205	0.134	-0.089	0.798

4.3. Performance metrics

The performance metrics used in this research include mean absolute error (MAE), mean square error (MSE) and root mean square error (RMSE). **Table 6** depicts the outcomes of the research.

- **RMSE**

It measures the average magnitude of prediction errors in the same units as the data, giving importance to higher errors because of the squared term. It provides an opportunity to assess how accurately the RLSTM model of biosensors predicts user emotional states and interactive behavior. Low RMSE values indicate a better fit between actual feedback and model output; this fit is crucial for the refinement of an interactive product.

- **MSE**

It measures the average of squared differences between actual values and predicted values, depicting overall model accuracy with large errors. It's very important for analyzing integration in biosensors and optimizing the performance of ISLO-RLSTM during iterative design. A lesser MSE ensures that the system functions well with diverse emotional and physiological states.

- **MAE**

It is the calculation of mean absolute prediction errors that give direct measures of deviations without highlighting the large ones. They are used in the verification of the consistency of predictions through real-time user interaction. Low MSE ensures biosensor-based systems do not let the system drift from user engagement by producing the correct interpretation of emotional feedback. The outcome of metrics is shown in **Table 6** and **Figure 6**.

Table 6. Outcome of ISLO-RLSTM model.

Performance Metrics	RMSE	MAE	MSE
ISLO-RLSTM [Proposed]	1.58	1.22	2.17

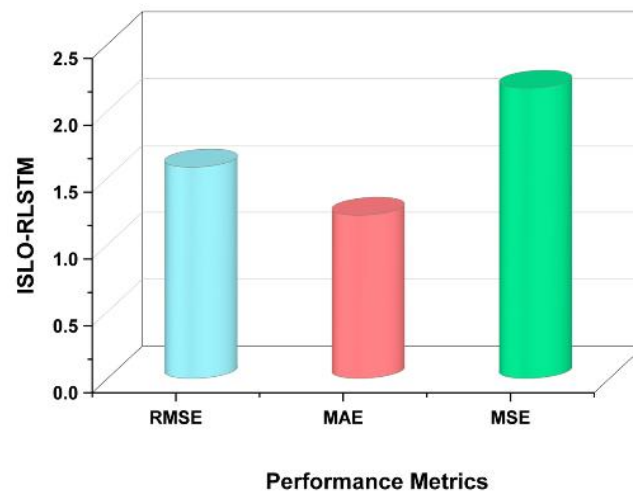


Figure 6. Outcomes of various metrics.

5. Discussion

The method's feasibility was demonstrated using a flavoring chair and teapot design, but more cultural and home product models need to be developed for designers. They investigated the association between frequency domain features and enjoyment under cultural components but only looked at frequency domain characteristics. An ISLO-RLSTM was employed for verification, but future research should evaluate the evolutionary impacts of the methods and optimize them for enhanced system effectiveness and quality of the product design. The flavoring chair and teapot shape were easily disassembled, and future studies should focus on creating a gene bank of morphological traits to improve goods. The present method creates two-dimensional wireframe patterns, but future work might include three-dimensional designs. The ISLO-RLSTM technique improves product design by optimizing biosensor data to make precise, real-time user experience predictions. This might be addressed in future research by expanding the process to incorporate three-dimensional designs, which would allow for a more realistic and immersive depiction of product conceptions. Such developments would provide designers with a greater understanding of consumer preferences and product functioning in addition to improving the designs' aesthetic appeal. Its adaptive learning enables consistent performance even with dynamic and noisy inputs.

6. Conclusion

The results of the EEG experiment demonstrated that the frontal alpha asymmetry, which was employed to gauge the participants' level of enjoyment when exposed to various cultural aspects, and the frontal α wave can represent the link between user emotion and product experience. By using this approach, designers might choose consumer preferences more objectively and steer clear of subjectivity when choosing cultural components. The perceptual location of creative and cultural items has been made possible by the user's perceptual image inquiry. Mastering the image sentiments of the users for creative and cultural items, as well as statistically

measuring the degree to which the user prefers image semantics, both of which are of benefit to the improvement of product form design and optimization.

To evolve product shapes, cultural elements from EEG experiments were used to code morphological characteristics, which were then crossed, mutated, and selected. Users' perceptual image vocabulary was evaluated to determine individual fitness values. ISLO-RLSTM has evaluated the user interaction by reducing fatigue from repeated interactions. As a result, the ISLO-RLSTM method performed better in RMSE at 1.58, MAE at 1.22, and MSE at 2.17. The evolutionary design system was created and validated using a flavored chair and teapot design example. Limitations include the expensive cost of biosensor integration and the difficulty in effectively interpreting different physiological data. The future scope includes creating cost-effective, scalable biosensor technologies and integrating AI to improve real-time adaptation and customization.

Author contributions: Conceptualization, JS and ISMY; software, MFBY; data curation, JS and ISMY; writing—original draft preparation, MFBY; writing—review and editing, JS and ISMY. All authors have read and agreed to the published version of the manuscript.

Ethical approval: Not applicable.

Conflict of interest: The authors declare no conflict of interest.

References

1. Nashruddin, S.N.A.B.M., Salleh, F.H.M., Yunus, R.M. and Zaman, H.B., 2024. Artificial Intelligence– Powered Electrochemical Sensor: Recent Advances, Challenges, and Prospects. *Heliyon*. <https://doi.org/10.1016/j.heliyon.2024.e37964>
2. Lei, Z.L. and Guo, B., 2022. 2D material-based optical biosensor: status and prospect. *Advanced Science*, 9(4), p. <https://doi.org/2102924.10.1002/advs.202102924>
3. Song, M., Lin, X., Peng, Z., Xu, S., Jin, L., Zheng, X. and Luo, H., 2021. Materials and methods of biosensor interfaces with stability. *Frontiers in Materials*, 7, p.583739. <https://doi.org/10.3389/fmats.2020.583739>
4. Bhatia, D., Paul, S., Acharjee, T. and Ramachairy, S.S., 2024. Biosensors and their widespread impact on human health. *Sensors International*, 5, p.100257. <https://doi.org/10.1016/j.sintl.2023.100257>
5. Verma, D., Singh, K.R., Yadav, A.K., Nayak, V., Singh, J., Solanki, P.R. and Singh, R.P., 2022. Internet of things (IoT) in nano-integrated wearable biosensor devices for healthcare applications. *Biosensors and Bioelectronics: X*, 11, p.100153. <https://doi.org/10.1016/j.biosx.2022.100153>
6. Tetyana, P., Shumbula, P.M. and Njengele-Tetyana, Z., 2021. Biosensors: design, development and applications. In *Nanopores*. IntechOpen. <https://doi.org/10.5772/intechopen.97576>
7. Purohit, B., Vernekar, P.R., Shetti, N.P. and Chandra, P., 2020. Biosensor nanoengineering: Design, operation, and implementation for biomolecular analysis. *Sensors International*, 1, p.100040. <https://doi.org/10.1016/j.sintl.2020.100040>
8. Su, Y., 2023. Visualization design of health detection products based on human-computer interaction experience in intelligent decision support systems. *Mathematical Biosciences and Engineering*, 20(9), pp.16725-16743.
9. Madrid, R.E., Ashur Ramallo, F., Barraza, D.E. and Chaile, R.E., 2022. Smartphone-based biosensor devices for healthcare: technologies, trends, and adoption by end-users. *Bioengineering*, 9(3), p.101. <https://doi.org/10.3390/bioengineering9030101>
10. Javaid, Z., Iqbal, M.A., Javeed, S., Maidin, S.S., Morsy, K., Shati, A.A. and Choi, J.R., 2024. Reviewing advances in nanophotonic biosensors. *Frontiers in Chemistry*, 12, p.1449161. <https://doi.org/10.3389/fchem.2024.1449161>
11. Alfaras, M., Primett, W., Umair, M., Windlin, C., Karpashevich, P., Chalabianloo, N., Bowie, D., Sas, C., Sanches, P., Höök, K. and Ersoy, C., 2020. Biosensing and actuation—Platforms coupling body input-output modalities for affective technologies. *Sensors*, 20(21), p.5968. <https://doi.org/10.3390/s20215968>

12. Zhou, Z., Tian, D., Yang, Y., Cui, H., Li, Y., Ren, S., Han, T. and Gao, Z., 2024. Machine learning assisted biosensing technology: An emerging powerful tool for improving the intelligence of food safety detection. *Current Research in Food Science*, p.100679. <https://doi.org/10.1016/j.crfs.2024.100679>
13. Zhu, Z., 2022. Integration of biosensors and deep learning for assessing food quality. *Authorea Preprints*. <https://doi.org/10.22541/au.166879033.33669472/v1>
14. Ding, Y., Sun, Y., Liu, C., Jiang, Q.Y., Chen, F. and Cao, Y., 2023. SeRS-Based Biosensors Combined with Machine Learning for Medical Application. *ChemistryOpen*, 12(1), p.e202200192. <https://doi.org/10.1002/open.202200192>
15. Anapanani, G., 2023. Machine Learning for Biosensors. West Virginia University. <https://doi.org/10.33915/etd.12118>
16. Schackart III, K.E. and Yoon, J.Y., 2021. Machine learning enhances the performance of bioreceptor-free biosensors. *Sensors*, 21(16), p.5519. <https://doi.org/10.3390/s21165519>
17. Yang, L., Shi, Z., Jia, R., Kou, J., Du, M., Bian, C. and Wang, J., 2024. Multi-branch deep learning neural network prediction model for the development of angular biosensors based on sEMG. *Frontiers in Bioengineering and Biotechnology*, 12, p.1492232. <https://doi.org/10.3389/fbioe.2024.1492232>
18. Bhaiyya, M., Panigrahi, D., Rewatkar, P. and Haick, H., 2024. Role of Machine Learning Assisted Biosensors in Point-of-Care-Testing For Clinical Decisions. *ACS sensors*, 9(9), pp.4495-4519. <https://doi.org/10.1021/acssensors.4c01582?urlappend=%3Fref%3DPDF&jav=VoR&rel=cite-as>
19. Mehrani, M., Attarzadeh, I. and Hosseinzadeh, M., 2020. Sampling rate prediction of biosensors in wireless body area networks using deep-learning methods. *Simulation Modelling Practice and Theory*, 105, p.102101. <https://doi.org/10.1016/j.simpat.2020.102101>
20. Hemdan, M., Ali, M.A., Doghish, A.S., Mageed, S.S.A., Elazab, I.M., Khalil, M.M., Mabrouk, M., Das, D.B. and Amin, A.S., 2024. Innovations in Biosensor Technologies for Healthcare Diagnostics and Therapeutic Drug Monitoring: Applications, Recent Progress, and Future Research Challenges. *Sensors (Basel, Switzerland)*, 24(16), p.5143. <https://doi.org/10.3390/s24165143>
21. Zhao, F., Wang, L., Li, M., Wang, M., Liu, G. and Ping, J., 2023. Nanozyme-based biosensor for organophosphorus pesticide monitoring: Functional design, biosensing strategy, and detection application. *TrAC Trends in Analytical Chemistry*, 165, p.117152. <https://doi.org/10.1016/j.trac.2023.117152>
22. Inshyna, N.M., Chorna, I.V., Primova, L.O., Hrebenyk, L.I. and Khyzhnia, Y.V., 2020. Biosensors: Design, classification and application. [https://doi.org/10.21272/jnep.12\(3\).03033](https://doi.org/10.21272/jnep.12(3).03033)